

## N O T I C E

THIS DOCUMENT HAS BEEN REPRODUCED FROM  
MICROFICHE. ALTHOUGH IT IS RECOGNIZED THAT  
CERTAIN PORTIONS ARE ILLEGIBLE, IT IS BEING RELEASED  
IN THE INTEREST OF MAKING AVAILABLE AS MUCH  
INFORMATION AS POSSIBLE

(NASA-CR-164216) AN INTERACTING LOOP MODEL  
OF SOLAR FLARE BURSTS (Stanford Univ.) 33 p  
HC A03/MF A01 CSCL 03B

N81-23005

Unclas  
G3/92 42122

# AN INTERACTING LOOP MODEL OF SOLAR FLARE BURSTS

by

A. Gordon Emslie

National Aeronautics and Space Administration  
Grant NGL 05-020-272  
Grant NAGW-92

Office of Naval Research  
Contract N00014-75-C-0673

SUIPR Report No. 831

March 1981



INSTITUTE FOR PLASMA RESEARCH  
STANFORD UNIVERSITY, STANFORD, CALIFORNIA

**AN INTERACTING LOOP MODEL OF SOLAR FLARE BURSTS**

by

**A. Gordon Emslie**

**National Aeronautics and Space Administration**

**Grant NGL 05-020-272**

**Grant NAGW-92**

**Office of Naval Research**

**Contract N00014-75-C-0673**

**SUIPR Report No. 831**

**March 1981**

**Institute for Plasma Research  
Stanford University  
Stanford, California**

## AN INTERACTING LOOP MODEL OF SOLAR FLARE BURSTS

A. Gordon Emslie

Institute for Plasma Research, Stanford University

Received

---

## ABSTRACT

We show how, as a result of the strong heating produced at chromospheric levels during a solar flare burst, the local gas pressure can transiently attain very large values in certain regions. The effectiveness of the surrounding magnetic field at confining this high pressure plasma is therefore reduced and the flaring loop becomes free to expand laterally. In so doing it may drive magnetic field lines into neighboring, non-flaring, loops in the same active region, causing magnetic reconnection to take place and triggering another flare burst. The features of this interacting loop model are found to be in good agreement with the energetics and time structure of flare-associated solar hard X-ray bursts.

Subject headings: hydromagnetics - plasmas - Sun : flares - Sun : X-rays

## I. INTRODUCTION

Solar hard X-ray bursts (photon energy  $\epsilon \geq 10$  keV) frequently exhibit detailed time structure on timescales of a few seconds (see, e.g., Hoyng, Brown, and van Beek 1976; Dennis, Frost, and Orwig 1981). This has led to the concept of the "Elementary Flare Burst" (EFB - van Beek, de Feiter, and de Jager 1974; de Jager and de Jonge 1978), whereby it is supposed that hard X-ray bursts with a complicated time structure involving several "spikes" are in fact composed of a number of discrete EFB's, each with a simple "rise-fall" time structure.

de Jager and de Jonge (1978) were the first to point out that there appears to be a significant difference (as measured by their FWHMs) amongst EFB's in a particular hard X-ray event, suggesting that different EFB's correspond to the successive activation of a number of different sources, rather than the continual reactivation of a single source. Karpen, Crannell, and Frost (1979) also studied the structure of hard X-ray bursts exhibiting clear EFB structure (in their nomenclature, "multiply impulsive" events), together with microwave data on the same bursts, and showed that the source parameters (density, temperature, magnetic field, etc.) for each EFB were markedly different. This similarly led them to the conclusion that different EFB's originate in different regions of the flare. Finally, Kane, Pick, and Raoult (1980) studied the spatial structure of type III radio bursts observed to be synchronous with hard X-ray EFB's and deduced that each of the hard X-ray bursts in the event in question (on 2 September 1978) originated in one of two spatially distinct regions, separated by some 7 minutes of arc, or  $3 \times 10^{10}$  cm.

There thus appears to be a significant amount of evidence for different EFB's corresponding to excitation of different parts of the flare region.

Kane, Pick and Raoult (1980), in attempting to explain their inferred spatial separation of the individual hard X-ray bursts, rule out chance coincidence of the two bursts occurring independently as being statistically improbable<sup>1</sup>, and point out that any signal from one region to the other would

---

<sup>1</sup> Kane, Pick, and Raoult (1980) quote an occurrence rate of  $\approx 10 \text{ day}^{-1}$  for the class of burst appropriate to their observations, and so deduce the probability of two bursts occurring within a five second time interval (the temporal separation of the bursts) to be  $\leq 10^{-7}$ . This is in fact the probability, based on Poisson statistics, of two bursts occurring in a given 5 second time interval. However, since the time of the first burst is arbitrary, one should actually calculate the probability of a single burst occurring in a given 5 second interval; this evaluates, using the same occurrence rate quoted by Kane, Pick, and Raoult, to be  $\approx 5 \times 10^{-4}$ , or about 1 in 2000. Although this is still a small number, it is conceivable, considering the large number of bursts observed, that chance coincidence may in fact have been the responsible agent in the event studied by Kane, Pick, and Raoult.

---

have to travel much faster than any reasonable Alfvén speed, thus ruling out a sympathetic trigger. They thus interpret their observations as implying activation of two different source regions by the same external disturbance, i.e. an energetic electron beam in a "thin target" (Datlowe and Lin 1973) scenario. However, in the event studied by Kane, Pick, and Raoult (1980), the two flaring regions are separated by a distance comparable to a solar radius, and

therefore clearly belong to different active regions; for two hard X-ray sources located in the same active region, a sympathetic trigger cannot be ruled out by such disturbance velocity considerations (see Karpen, Crannell, and Frost 1979). In this paper we propose a means of producing just such a trigger.

To date, all models of the response of the solar atmosphere to a flare energy input have been one-dimensional in nature. This simplifying characteristic is usually justified by noting that for typical parameters in the flaring corona and chromosphere the quantity  $\beta$ , defined as the ratio of gas to magnetic pressures, is much less than unity, so that the plasma is constrained to move along the magnetic field lines. (The assumption of  $\beta \ll 1$  breaks down near the photosphere [number density  $n \geq 10^{16} \text{ cm}^{-3}$ ], but such deep layers of the atmosphere remain relatively undisturbed during the flare [Machado, Emslie, and Brown 1978].) However, the relation  $\beta \ll 1$  follows from consideration of steady-state conditions; as we shall show below (§II) the fact that the timescales for impulsive heating, and for hydrodynamic relaxation, of the solar chromosphere are markedly different can result in the formation of regions of transiently very large gas pressure, in which  $\beta$  is comparable with unity. While to explore fully the resulting three-dimensional time-dependent response of the solar atmosphere to the flare energy input is beyond the scope and purpose of the present paper, we shall discuss semi-quantitatively the effect of creating such a transient high- $\beta$  regime. In particular, we shall demonstrate (§III) how this high gas pressure region causes the energized flare loop to expand laterally, dragging the (frozen-in) magnetic field lines with the plasma. A magnetohydrodynamic disturbance is thus established, which can

subsequently interact with the field lines of a neighboring quasi-static loop in the same solar active region, causing magnetic reconnection and further release of energy, thus triggering the next EFB. This process can be continued amongst the various loops in the preflare active region complex, producing the "multiple-spike" X-ray flux versus time profile characteristic of so many events (Hoyng, Brown, and van Beek 1976; Karpen, Crannell, and Frost 1979). The energetics and timescales of this process are explored in §III, and it is shown that both are compatible with their counterparts inferred from hard X-ray data. In §IV we state our conclusions and suggest areas for more detailed research.

## II. FORMATION OF REGIONS OF TRANSIENTLY HIGH GAS PRESSURE DURING THE IMPULSIVE HEATING PHASE OF A FLARE BURST

There is some controversy as to the exact mechanism responsible for heating the solar chromosphere during flares, candidates including non-thermal electron bombardment (Brown 1973; Lin and Hudson 1976; Emslie 1980), soft X-ray irradiation (Somov 1975; Héroux and Nakagawa 1977, 1978; Machado 1978; Hyder 1981), and dissipation of hydrodynamic (Craig and McClymont 1976) and thermal (Smith and Harmony 1981) shocks. For the purposes of the present discussion we shall concentrate on the first of these, for two reasons. First, our discussion will relate to events with a strong hard X-ray signature; to date all models (both "thermal" and "non-thermal"; see Emslie and Rust 1979) of the hard X-ray production mechanism involve a substantial amount of the

flare energy to be in the form of a beam of precipitating high energy electrons (see, e.g., Brown 1971; Melrose and Brown 1976; Brown, Melrose, and Spicer 1979; Vlahos and Papadopoulos 1979; Emslie and Vlahos 1980; Smith and Brown 1980). Second, and more importantly for our present study, this mechanism of chromospheric heating has been extensively studied in the literature; in particular, calculations of the detailed time-dependent response of the solar atmosphere to such a beam of non-thermal electrons have been carried out by a number of authors (Kostyuk and Pikel'ner 1975; Sermulina et al. 1980; Somov, Syrovatskii, and Spektor 1981).

Early work on the response of the solar chromosphere to a hypothetical flare energy input was, for reasons of simplicity and tractability, confined to a discussion of steady-state model atmospheres (e.g., Brown 1973; Henoux and Nakagawa 1977, 1978; Brown Canfield, and Robertson 1978; LaBonte 1978). Kostyuk and Pikel'ner (1975) attempted a time-dependent calculation of the hydrodynamic response of the solar atmosphere to a sustained ( $\approx 100$  s) injection of non-thermal electrons. However, they did not adequately treat the problem of radiative instability of the heated plasma; further, their published results lack important information, such as density profiles (see Canfield et al. 1980). Recently more detailed work on the time-dependent response of the atmosphere to an injected beam of non-thermal electrons has been carried out (Sermulina et al. 1980; Somov, Syrovatskii, and Spektor 1981). Due to numerical difficulties, these analyses are restricted to only short ( $\leq 10$  second) bursts of heating, and subsequent relaxation of the energized atmosphere to its pre-flare state. This timescale is, however, quite acceptable for studying events composed of discrete EFB's (de Jager and de Jonge 1978;

Karpen, Crannell, and Frost 1979). Further, the results clearly show that in all cases the electron temperature of the preflare chromospheric material is heated to coronal temperatures in times on the order of one second, while the density of this material stays relatively constant, due to the much longer hydrodynamic time scale. Knowledge of the detailed behavior of the atmosphere long after this impulsive rise in electron temperature is not necessary for the subsequent discussion.

Figure 1 Figure 1 (from Somov, Syrovatskii, and Spektor 1981) shows the density  $n$  ( $\text{cm}^{-3}$ ) and electron temperature  $T_e$  (K) as a function of column density  $N$  ( $\text{cm}^{-2}$ ) after 5 seconds of heating by a beam of non-thermal electrons with an injected energy flux spectrum (electrons  $\text{cm}^{-2}\text{s}^{-1}$  per unit energy) in the form of a truncated power law:

$$F_0(E_0) = (\delta - 2) \frac{\mathcal{F}}{E_1^2} \left( \frac{E_0}{E_1} \right)^{-\delta} ; E_0 > E_1, \quad (1)$$

where  $\delta = 3$ ,  $E_1 = 10$  keV, and  $\mathcal{F}$  (the total injected energy flux) =  $10^{11}$  ergs  $\text{cm}^{-2}\text{s}^{-1}$ . The behaviors of  $n$  and  $T_e$  in the (hydrostatic) preflare atmosphere are shown dashed. Note that in this preflare state  $T_e$  is constant (= 6700 K) and  $n$ , consequently, has an exponential variation with height (so that  $n \propto N$ ). This initial state is admittedly somewhat unphysical; however, it turns out (Somov, Syrovatskii, and Spektor 1981) that the detailed structure of the preflare atmosphere at low column densities (great heights) is not an important consideration. This is because at such low column densities the flare energy input is much larger than any preflare energy source or sink (see Emslie 1980), so that the plasma is explosively heated, resulting in a final structure which is essentially independent of the assumed initial

conditions. At greater column densities (below the region of explosive heating -- see Brown 1973), the preflare and flare energy inputs are more comparable, and due consideration must be given to the initial conditions of the atmosphere. Somov, Syrovatskii, and Spektor's (1981) assumed value of  $T_e = 6700$  K reflects this point, since this is a typical temperature for the upper chromosphere (see Machado et al. 1980). Clearly a more detailed description of  $T_e(N)$  for large  $N$  would be desirable in order to more accurately assess the structure of the flaring chromosphere at these levels. However, this paper will be concerned only with the structure of the atmosphere in the explosively heated region, and so we shall not dwell on this matter further.

Also shown in Figure 1 is the flaring pressure

$$P = nT_e \text{ cm}^{-3} \text{ K} \quad (2)$$

and the equipartition magnetic field strength

$$B_{eq} = (8\pi kP)^{1/2} \text{ G}, \quad (3)$$

where  $k$  is Boltzmann's constant. In writing eq. (2), we have neglected the contribution from the ions, since  $T_i \ll T_e$  (Somov, Syrovatskii, and Spektor 1981). It is clear from the figure that a region of greatly enhanced gas pressure is formed in the range  $10^{19} \leq N \leq 4 \times 10^{19} \text{ cm}^{-2}$ . For  $10^{19} \leq N \leq 2 \times 10^{19} \text{ cm}^{-2}$  this is the result of a sudden increase in temperature over preflare values (the density remaining essentially unchanged), while for  $2 \times 10^{19} \text{ cm}^{-2} \leq N \leq 4 \times 10^{19} \text{ cm}^{-2}$  the excess pressure is attributable to a density enhancement, brought upon by compression due to the overlying high pressure material. This region of enhanced density is very thin, being only  $\Delta N/n = 2$  km thick, and is a characteristic feature of the chromospheric side of a

(transient) flare-induced transition region. When heated it expands at constant pressure to form a region with the original preflare density and a new hotter, temperature, and a new region of enhanced density is created somewhat deeper in the atmosphere. As the heating proceeds, this layer (and so the transition region) "burns" its way deeper and deeper into the atmosphere. This process stops when the heat being deposited on the chromospheric side of this region has been reduced, by attenuation of the electron flux by the overlying material, to such an extent that it can no longer overcome the ability of the plasma to radiate the energy away. The plasma is now unable to enter the temperature regime of radiative instability (see Field 1965; Fox and Tucker 1969) and so heat up to coronal temperatures ( $\approx 10^7$  K). The atmosphere thus remains approximately in this state (ignoring heat redistribution due to thermal conduction and radiative transfer) until the cessation of the electron energy input, at which point it starts to relax back, through both thermal conduction and radiation, to its preflare state.

Although the results of Somov, Syrovatskii, and Spektor (1981) are rather specific, we may use the physical insight gained in the above discussion to generalize their results to other cases. The level  $N_{TR}$  of the transition region will be determined by the total amount of energy available for heating material to coronal temperatures, while the magnitude of the gas pressure in the transient regime at this newly-formed transition region will be approximately given by

$$P = P_0 \frac{T_c}{2T_{ch}}, \quad (4)$$

where  $P_0$  is the initial pressure at  $N = N_{TR}$ ,  $T_c$  and  $T_{ch}$  are the coronal and chromospheric electron temperatures ( $\approx 10^7$  K and  $10^4$  K) respectively, and the factor 2 in the denominator follows from the fact that  $T_e > T_i$  during the impulsive phase of the flare, while  $T_e = T_i$  in the preflare chromosphere.

We now proceed to estimate  $N_{TR}$  from simple theoretical considerations. The heating rate ( $\text{ergs cm}^{-3}\text{s}^{-1}$ ) due to Coulomb collisions of a beam of non-thermal electrons, injected vertically with energy spectrum  $F_0(E_0)$  is (Brown 1973; Emslie 1978--we ignore the effect of reverse current ohmic losses in the impulsive phase [see Emslie 1980, 1981])

$$I_B(N) = Kn \int_{E^*}^{\infty} \frac{F_0(E_0) dE_0}{E_0 (1-3KN/E_0^2)^{2/3}}, \quad (5)$$

where  $K = 2\pi e^4 \Lambda$  ( $e$  = electronic charge [e.s.u.],  $\Lambda$  = Coulomb logarithm), and

$$E^* = \max(E_1, [3KN]^{1/2}), \quad (6)$$

$E_1$  being the low energy cutoff to the injected beam energy spectrum--see eq.

(1). The total heating rate ( $\text{ergs cm}^{-2}\text{s}^{-1}$ ) down to column depth  $N$  is thus

$$J_B(N) = \int_0^N I_B(N') \frac{dz}{dN'} dN' = \int_0^N \frac{I_B(N') dN'}{n}, \quad (7)$$

or, using eqs. (1) and (5),

$$J_B(N) = K (\delta-2) \int_{E_1}^{\infty} E_0^{\delta-2} \int_{N'=0}^N \int_{E_0=E^*}^{\infty} \frac{dE_0 dN'}{E_0^{\delta+1} (1-3KN'/E_0^2)^{2/3}}. \quad (8)$$

For  $N < N_1 = E_1^2/3K$ , we have  $E^* = E_1$ ; reversing the order of integration then yields

$$J_B(N) \Big|_{N < N_1} = \mathcal{F} \left[ 1 - (\delta-2)E_1^{\delta-2} \int_{E_1}^{\infty} E_0^{1-\delta} (1-3KN/E_0^2)^{1/3} dE_0 \right]. \quad (9)$$

Setting  $E_0 = E_1 \sec \theta$  reduces  $J_B(N)$  to a form convenient for computation:

$$J_B(N) \Big|_{N < N_1} = \mathcal{F} \left[ 1 - (\delta-2) \int_0^{\pi/2} \cos^{\delta-3} \theta (1 - v \cos^2 \theta)^{1/3} \sin \theta d\theta \right], \quad (10)$$

where

$$v = \frac{3KN}{E_1^2} = \frac{N}{N_1}. \quad (11)$$

For  $N > N_1$ ,  $E^* = (3KN)^{1/2}$ ; thus, in evaluating  $J_B(N)$  for  $N > N_1$ , we must split the integral over  $N'$  into two parts--one from  $N' = 0$  to  $N' = N_1$  and the other from  $N' = N_1$  to  $N' = N$ . The first part,  $J_{B1}$ , is given by equation (10) with  $v = 1$ , viz.

$$J_{B1} = \mathcal{F} \left[ 1 - \frac{1}{3} B\left(\frac{\delta}{2}, \frac{1}{3}\right) \right], \quad (12)$$

where  $B$  is the Beta function (see Abramowitz and Stegun 1965, p. 258). The second term,

$$J_{B2}(N) = (\delta-2)\mathcal{F} E_1^{\delta-2} \int_{N'=N_1}^N \int_{E_0=(3KN')^{1/2}}^{\infty} \frac{dE_0 dN'}{E_0^{\delta+1} (1-3KN'/E_0^2)^{2/3}}, \quad (13)$$

can be evaluated in a straightforward manner to give (see Emslie, Brown, and Donnelly 1978)

$$J_{B2}(N) = \frac{1}{3} B\left(\frac{\delta}{2}, \frac{1}{3}\right) \mathcal{F}\left[1 - (N/N_1)^{1 - \frac{\delta}{2}}\right] \quad (14)$$

Finally, adding equations (12) and (14) gives

$$J_B(N) \Big|_{N \gg N_1} = \mathcal{F}\left[1 - \frac{1}{3} B\left(\frac{\delta}{2}, \frac{1}{3}\right) (N/N_1)^{1 - \frac{\delta}{2}}\right]; \quad (15)$$

note that this result can also be obtained by using the identity

$$\mathcal{F} = J_B(\infty) = J_B(N) + \int_N^{\infty} \frac{I_B(N') dN'}{n}, \quad (16)$$

where the second term is evaluated in a straightforward manner with  $E^* = (3KN')^{1/2}$ .

Equations (10) and (15) are the results needed to continue our analysis.

In the case  $\delta = 4$  (a not unreasonable value--see Hoyng, Brown, and van Beek 1976) they reduce to the simple expressions

$$J_B(N) = \begin{cases} \mathcal{F}\left\{1 - \frac{3N_1}{4N} \left[1 - \left(1 - \frac{N}{N_1}\right)^{4/3}\right]\right\}; & N \leq N_1 \\ \mathcal{F}\left(1 - \frac{3N_1}{4N}\right) & ; N \gg N_1 \end{cases} \quad (17)$$

We shall use these expressions hereafter. The effect of varying  $\delta$  will be considered briefly below.

Now consider a beam injected for a time  $\tau$ , which deposits its energy above column depth  $N_{TR}$  and heats this material from chromospheric to coronal temperatures. Energy balance in the region  $N < N_{TR}$  thus dictates that

$$J_B(N_{TR}) \tau = N_{TR} k(T_C - T_{ch}) \approx N_{TR} k T_C, \quad (18)$$

where we have ignored energy losses due to thermal conduction and radiation (cf. above); this neglect will cause the  $N_{TR}$  calculated from eq. (18) to be an upper limit. For  $E_1 = 10$  keV (see Somov, Syrovatskii, and Spektor 1981),  $N_1 = 10^{19} \text{ cm}^{-2}$  (Emslie 1978); thus, by appealing to Somov, Syrovatskii, and Spektor's (1981) results, we may take  $N_{TR} > N_1$  (we shall in fact verify this assumption a posteriori). Using eq. (17) in eq. (18) then yields

$$1 - \frac{1}{x} = \frac{3\zeta}{4} x, \quad (19)$$

where

$$x = \frac{4N_{TR}}{3N_1}; \quad \zeta = \frac{N_1 k T_C}{f \tau}. \quad (20)$$

Equation (19) solves to give

$$x = \frac{2}{3\zeta} [1 + (1 - 3\zeta)^{1/2}], \quad (21)$$

where the positive sign in the square brackets has been chosen, so that as  $f \rightarrow \infty$  ( $\zeta \rightarrow 0$ ),  $N_{TR} > N_1$ . In terms of physical variables, eq. (21) is

$$N_{TR} = \frac{\mathcal{F}\tau}{2kT_c} \left\{ 1 + \left[ 1 - 3N_1 kT_c / \mathcal{F}\tau \right]^{1/2} \right\}. \quad (22)$$

Now, by eq. (4), the transient (i.e. flaring) pressure at this level is given by

$$P = \frac{N_{TR} m_H g_\odot T_c}{2kT_{ch}}, \quad (23)$$

where  $m_H$  is the hydrogen mass and  $g_\odot$  the solar gravity. Substituting for  $N_{TR}$  from eq. (22) and inserting numerical values gives

$$P = 6 \times 10^{11} \frac{\mathcal{F}\tau}{T_{ch}} \left\{ 1 + \left[ 1 - \frac{41.4E_1^2 T_c}{\mathcal{F}\tau} \right]^{1/2} \right\}. \quad (24)$$

We may now compare this expression with the results of Somov, Gyrovatskii, and Spektor (1981); see Figure 1. Ignoring the discrepancy in the value of  $\delta$  used (for other  $\delta$  in the range 3-6 the integrals in eqs. [10] and [13] may be evaluated numerically [or analytically] to yield results which differ from those for  $\delta = 4$  by only some 10%), we find from eq. (22), with  $\mathcal{F} = 10^{11} \text{ ergs cm}^{-2} \text{ s}^{-1}$ ,  $E_1 = 10 \text{ keV}$ ,  $\tau = 5 \text{ s}$ ,  $T_{ch} = 10^4 \text{ K}$ , and  $T_c = 10^7 \text{ K}$ , that

$$N_{TR} = 1.8 \times 10^{20} \text{ cm}^{-2} \quad (25)$$

(note that this is indeed greater than  $N_1$ , as was earlier assumed). Further, eq. (24) gives

$$P = 6 \times 10^{19} \text{ cm}^{-3} \text{ K}, \quad (26)$$

corresponding to (eq. [3])

$$B_{eq} = 450 \text{ G} . \quad (27)$$

Although these values are somewhat larger than the values given by Somov, Syrovatskii, and Spektor (1981) (see Figure 1), we note that the value of  $N_{TR}$  in eq. (25) is more compatible with empirical estimates of this quantity (Machado et al. 1980), possibly indicating deficiencies in the calculations of Somov, Syrovatskii, and Spektor (Emslie, Brown, and Machado 1981). Even allowing for the fact that our estimates of  $N_{TR}$  are necessarily upper limits, due to the oversimplistic energy balance equation (18), it nevertheless appears, therefore, that the gas pressure  $P$  can easily attain transient values of order  $10^{19} \text{ cm}^{-3} \text{ K}$  during the impulsive phase of flares, corresponding to an equipartition magnetic field strength  $B_{eq} = 200 \text{ G}$ . (For example, increasing  $\tau$  to 10s in the calculations of Somov, Syrovatskii, and Spektor [1981] should increase  $B_{eq}$  by a factor  $\approx 2^{1/2}$  over the values in Figure 1.)

These values of  $B_{eq}$  are not small compared to the ambient field strength in the chromosphere. Thus it appears that the assumption of a plasma constrained to move along preexisting field lines is not adequate in describing the impulsive phase of a solar flare burst, since there is no longer an overwhelming force (due to magnetic pressure) restricting motion perpendicular to these field lines. In the next section we shall discuss the implications of this situation for the evolution of the flare.

## III. THE INTERACTION OF NEIGHBORING LOOPS

Figure 2

Consider now the situation depicted in the left sketch of Figure 2, which shows two typical loops in an active region loop complex with a simple bipolar magnetic field topology. (For clarity, the field lines between and around loops  $L_1$  and  $L_2$  are not shown.) At some instant loop  $L_1$  becomes unstable (due to, for example, the formation of multiply connected magnetic islands in the loop [Spicer 1976, 1977] or the emergence of new flux at its base [Heyvaerts, Priest, and Rust 1977]) and flares, as indicated by the star at the loop apex. This causes a burst of hard X-ray emission to occur. Energy is transported along the loop and deposited at the dense footpoints, causing a transient strong pressure buildup (§II). Since the solar atmosphere is highly conducting, the field and plasma are "frozen" together, and so the large pressure gradient between the inside and outside of  $L_1$  drives a lateral expansion of the field lines defining loop  $L_1$ . (Of course, there are in addition motions along loop  $L_1$  driven by longitudinal pressure gradients [see Craig and McClymont 1976].) Although a full three-dimensional magnetohydrodynamic treatment of this expansion process is beyond the scope of the present paper (see §IV for further discussion), to order of magnitude one may assume that a disturbance of the surrounding field lines proceeds horizontally at the ion sound speed  $c_s = (kT_e/m_H)^{1/2}$ , which is approximately equal to the Alfvén speed  $v_A = B/(4\pi n m_H)^{1/2}$  since the gas and magnetic pressures are comparable (Figure 1). After a time  $\tau$  the disturbance encounters the neighboring loop  $L_2$  (Figure 2), allowing  $L_2$  to release its stored free energy (in the form of currents) through interaction with the disturbed field lines in a

neutral-sheet-type configuration (see Sturrock 1968), and giving rise to another burst of hard X-ray emission, spatially distinct from the location of the first burst (see §I).

In order for the phenomenon just described to explain the features of EFB's, the interaction time  $\tau$  must be roughly equal to the temporal separation  $\tau_{\text{EFB}}$  of EFB's. Thus, the lateral separation  $D$  of the loops  $L_1$  and  $L_2$  must be of order

$$D \approx V_A \tau_{\text{EFB}} , \quad (28)$$

which, setting  $\tau_{\text{EFB}} = 5 - 10$  s (de Jager and de Jonge 1978) and  $V_A = 5 \times 10^7$  cm s<sup>-1</sup> (using  $B = 500$  G and the density values shown in Figure 1), gives

$$D \approx (3 - 5) \times 10^8 \text{ cm} , \quad (29)$$

an entirely reasonable value.

The situation envisaged ("driven merging flux") is somewhat similar to that in the flare model by Gold and Hoyle (1960), or in the emerging flux model of Heyvaerts, Priest, and Rust (1977). However, there are some significant differences, as Figure 2 shows. Because the two loops under consideration are part of the same active region complex, which we assume to have a simple bipolar structure, the polarities of the corresponding footpoints of the two loops are the same; such a situation gives no reversal of the toroidal (i.e. longitudinal) component of the magnetic field at the contact plane between  $L_1$  and  $L_2$  and so this toroidal component of the field cannot be responsible for any subsequent energy release as in the model of Heyvaerts, Priest,

and Rust (1977). Further, the (poloidal) currents corresponding to these toroidal fields are antiparallel in the contact plane and therefore repel, instead of attracting in the (field-reversed) Gold and Hoyle (1960) model. However, by the same considerations, any twist (i.e., departure from a potential configuration) of the magnetic field lines will be in the same sense as viewed by a remote observer, which leads to a reversal of the poloidal components of the magnetic field in the contact plane, providing a situation suitable for reconnection of this poloidal component in a neutral-sheet-type scenario (see Sturrock 1968). The force required to overcome the repulsion of the poloidal currents is the hydrodynamic pressure of the heated transition region in the flaring loop; a simple calculation shows that the condition  $\beta = 1$  is equivalent to the condition that the gas pressure gradient can overcome the electrical repulsion of these poloidal currents.

This "poloidal flux annihilation" aspect of the present model gives, upon further consideration, some rather pleasing results. First, since the toroidal component of the magnetic field remains intact after the reconnection process, the basic spatial configuration of the loops remain intact, permitting the formation of the soft X-ray emitting post-flare loops frequently observed (e.g., Pallavicini, Serio, and Vaiana 1977). Second, during the reconnection  $\partial \mathbf{B} / \partial t$ , and so  $\nabla \times \mathbf{E}$ , is in the poloidal direction. This gives an induced  $\mathbf{E}$  vector which is predominantly toroidal, i.e., parallel to the remaining magnetic field lines, thus allowing efficient acceleration of particles along these field lines. (In standard neutral-sheet-type models [e.g., Sturrock 1968]  $\partial \mathbf{B} / \partial t$  and  $\nabla \times \mathbf{E}$  are mainly vertical, resulting in an induced  $\mathbf{E}$  vector which is horizontal, i.e., perpendicular to the remaining [closed] field

lines.) Third, there is no need for a complex magnetic topology at the loop footpoints, such as is required by both the Gold and Hoyle (1960) model and the emerging flux model of Heyvaerts, Priest, and Rust (1977).

One may also estimate the energy released in the annihilation of this poloidal flux. Assuming a twist of  $\approx \pi$  in each flux tube (see Barnes and Sturrock 1972), a toroidal field strength of some 300 G (see above), and a footpoint area  $A = D^2 = 3 \times 10^{17} \text{ cm}^2$ , we find that the total energy released is

$$E_{\text{rel}} = \frac{\epsilon^2 B^2 D^2 L}{8\pi} \left(\frac{D}{L}\right)^2, \quad (30)$$

where  $L$  is the length of the flux tube ( $\approx 3 \times 10^9 \text{ cm}$ ) and  $\epsilon$  is the fraction of the poloidal field that is destroyed. Now, the proposed model relies on the fact that  $\epsilon < 1$ , since some poloidal flux must remain after each loop "encounter" if the "domino" effect leading to successive EFB's is to work. Thus, setting  $\epsilon = 1/3$ ,  $B = 500 \text{ G}$ ,  $D = 5 \times 10^8 \text{ cm}$ , and  $L = 3 \times 10^9 \text{ cm}$ , we obtain

$$E_{\text{rel}} = 3 \times 10^{28} \text{ ergs}. \quad (31)$$

We may compare this with the energy required to produce a single hard X-ray EFB. Hard X-ray spectra in moderately large flares may be represented well by the power-law form

$$I(\epsilon) = a\epsilon^{-\gamma} \text{ photons cm}^{-2} \text{ s}^{-1} \text{ keV}^{-1}, \quad (32)$$

with  $a = 10^6$  and  $\gamma (= \delta - 1) = 3 - 4$  (see Hoyng, Brown, and van Beek 1976). To

produce such a burst by thick target bremsstrahlung of a beam of high energy electrons requires an injection rate of electrons with energies  $> 25$  keV of

$$F_{25} = 4 \times 10^{33} a(\gamma-1)^2 B(\gamma^{1/2}, 1/2) (25)^{-\gamma} = 10^{35} - 10^{36} \text{ electrons s}^{-1} \quad (33)$$

(Hoyng, Brown, and van Beek 1976), corresponding to a total injected power

$$P = \frac{\gamma}{\gamma-1} F_{25} \times 25 \text{ keV} = 3 \times 10^{27} - 3 \times 10^{28} \text{ erg s}^{-1}. \quad (34)$$

Comparing eqs. (31) and (34) with a FWHM for the EFB of  $\approx 5$ s (de Jager and de Jonge 1978) indicates agreement to within an order of magnitude, which considering the crudeness of the above argument, is quite acceptable.

This completes the scenario of the interacting loop model, whose energetics and timescales have been shown to agree well with observations. In the final section we shall discuss some features of the model in greater detail, and also point out areas for future work.

#### IV. DISCUSSION

The analysis of the preceding two sections is of course somewhat schematic, and is intended only to provide a general description of the main features of the model. Nevertheless, it not only accounts for the EFB description of hard X-ray bursts, but also, for plausible parameters, successfully accounts for both the observed intensity and temporal spacing of EFB's. The

only a priori requirements of the model are (i) the initial energy release in one of the active region loops ( $L_1$  in Figure 2), which may occur by any of the currently proposed mechanisms (e.g., the tearing mode instability in a stressed arch geometry--Spicer 1976, 1977; van Hoven 1979), and (ii) the existence of a large scale current pattern in the active region, to provide the poloidal flux component which is annihilated in the "domino" process of successive energy releases.

Clearly many aspects of the model require more detailed study. For example, in Figure 2 it is tacitly assumed that the energized flux tube expands along its entire length as a result of the gas pressure forces which are localized at its base. Our intuitive justification for this is that the tension in the magnetic lines of force will tend to "straighten out" any "bulge" formed by a local expansion of the field; however, the timescale for the entire loop to respond to this tensile force will be of order  $L/V_{A, \text{corona}}$ , which for very large ( $L/D$ ) may be larger than the inter-loop collision timescale  $\tau_c$  (eq. [29]), even allowing for the reduced density, and corresponding higher Alfvén velocity, in the corona. A full three-dimensional magnetohydrodynamic analysis of the situation is clearly necessary to resolve this issue satisfactorily, just as it is also required to adequately model the expansion of the flux tube in the (difficult)  $\beta \approx 1$  regime (see remarks at the beginning of §III).

In addition to these issues, the details of the interaction between "colliding" flux tubes (see Figure 2) needs to be explored more fully. This requires study of driven magnetic reconnection processes, such as have been discussed previously, for the case of flux driven by magnetic buoyancy, by

Heyvaerts, Priest, and Rust (1977), and by references therein. This will enable us to better determine the temporal and spatial characteristics of the energy release in the quiescent loop (loop  $L_2$  in Figure 2).

I thank J. Leach for stimulating discussions which led to the ideas developed in this paper, A. N. McClymont for useful discussions regarding the hydrodynamics of the solar atmosphere during flares, and S. K. Antiochos and P. A. Sturrock for their comments on the manuscript. The author has benefited from discussions held at the Study of Energy Release in Flares (SERF) Workshop held at Stanford in August, 1980; this workshop was sponsored by the National Science Foundation and by the Scientific Committee on Solar-Terrestrial Physics (SCOSTEP). Financial support from grants NASA NGL 05-020-272, NASA NAGW-92, and contract ONR N00014-75-C-0673, is also gratefully acknowledged.

## REFERENCES

- Abramowitz, M., and Stegun, I. A. 1965, Handbook of Mathematical Functions  
(National Bureau of Standards).
- Barnes, C.W., and Sturrock, P. A. 1972, Ap. J., 174, 659.
- Brown, J. C. 1971, Solar Phys., 18, 489.
- \_\_\_\_\_ . 1973, Solar Phys., 31, 143.
- Brown, J. C., Canfield, R. C., and Robertson, M. N. 1978, Solar Phys., 57, 399.
- Brown, J. C., Melrose, D. B., and Spicer, D. S. 1979, Ap. J., 228, 592.
- Canfield, R. C., et al. 1980, in Solar Flares - A Monograph from Skylab Solar Workshop II, ed. P. A. Sturrock (Boulder; Colorado Associated Press),  
p. 231.
- Craig, I.J.D., and McClymont, A. N. 1976, Solar Phys., 50, 133.
- Cox, D. P., and Tucker, W. H. 1969, Ap. J., 157, 1157.
- Datlowe, D. W., and Lin, R. P. 1973, Solar Phys., 32, 459.
- de Jager, C., and de Jonge, G. 1978, Solar Phys., 58, 127.
- Dennis, B. R., Frost, K. J., and Orwig, L. E. 1981, Ap. J. (Letters), in press.
- Emslie, A. G. 1978, Ap. J., 224, 241.
- \_\_\_\_\_ . 1980, Ap. J., 235, 1055.
- \_\_\_\_\_ . 1981, Ap. J., submitted.
- Emslie, A. G., Brown, J. C., and Donnelly, R. F. 1978, Solar Phys., 57, 175.
- Emslie, A. G., Brown, J. C., and Machado, M. E. 1981, Ap. J., 246, in press.
- Emslie, A. G., and Rust, D. M. 1979, Solar Phys., 65, 271.
- Emslie, A. G., and Vlahos, L. 1980, Ap. J., 242, 359.
- Field, G. B. 1965, Ap. J., 142, 531.
- Gold, T., and Hoyle, F. 1960, M.N.R.A.S., 120, 89.
- Hénoux, J.-C., and Nakagawa, Y. 1977, Astr. Ap., 57, 105.
- \_\_\_\_\_ . 1978, Astr. Ap., 66, 385.

- Heyvaerts, J., Priest, E. R., and Rust, D. M. 1977, Ap. J., 216, 123.
- Hoyng, P., Brown, J. C., and van Beek, H. F. 1976, Solar Phys., 48, 197.
- Hyder, C. L. 1981, in preparation.
- Kane, S. R., Pick, M., and Raoult, A. 1980, Ap. J. (Letters), 241, L113.
- Karpen, J. T., Crannell, C. J., and Frost, K. J. 1979, Ap. J., 234, 370.
- Kostyuk, N. D., and Pikel'ner, S. B. 1975, Soviet Astron. - AJ, 18, 590.
- LaBonte, B. J. 1978, Big Bear Solar Observatory preprint #0173.
- Lin, R. P., and Hudson, H. S. 1976, Solar Phys., 50, 153.
- Machado, M. E. 1978, Solar Phys., 60, 341
- Machado, M. E., Avrett, E. H., Vernazza, J. E., and Noyes, R. W. 1980, Ap. J., 242, 336.
- Machado, M. E., Emslie, A. G., and Brown, J. C. 1978, Solar Phys., 58, 363.
- Melrose, D. B., and Brown, J. C. 1976, M.N.R.A.S., 176, 15.
- Pallavicini, R., Serio, S., and Vaiana, G. S. 1977, Ap. J., 216, 108.
- Sermulina, B. J., Somov, B. V., Spektor, A. R., and Syrovatskii, S. I. 1980, in IAU Symposium 91, Solar and Interplanetary Dynamics, eds. M. Dryer and E. Tandberg-Hanssen (Dordrecht: Reidel).
- Smith, L. F., and Brown, J. C. 1980, Ap. J., 242, 799.
- Smith, D. F., and Harmony, D. W. 1981, in preparation; abstract in B.A.A.S., 12, 893.
- Somov, B. V. 1975, Solar Phys., 42, 235
- Somov, B. V., Syrovatskii, S. I., and Spektor, A. R. 1981, Solar Phys., in press.
- Spicer, D. S. 1976, NRL Report 8036.
- \_\_\_\_\_ . 1977, Solar Phys., 53, 305.
- Sturrock, P. A. 1968, in IAU Symposium 35, Structure and Development of Solar Active Regions, ed. K. O. Kiepenheuer (Dordrecht: Reidel), p. 471.

van Beek, H. F., de Feiter, L., and de Jager, C. 1974, Space Research, XIV, 447

van Hoven, G. 1979, Ap. J., 232, 572.

Vlahos, L., and Papadopoulos, K. 1979, Ap. J., 233, 717.

## FIGURE CAPTIONS

Fig. 1. - Variation of density  $n$  ( $\text{cm}^{-3}$ ) and electron temperature  $T_e$  (K) with column density  $N$  ( $\text{cm}^{-2}$ ), from the Somov, Syrovatskii, and Spektor (1981) calculations of the hydrodynamic response of the solar chromosphere to an energy input in the form of a beam of non-thermal electrons. The preflare values of  $n$  and  $T_e$  are shown dashed; see §II for a discussion of these initial conditions. The values in the flare correspond to a time 5 seconds after the start of the heating and correspond to the largest enhancements in their calculations. The ion temperature  $T_i$  (not shown) is much less than  $T_e$ . Also shown is the pressure  $P = nT_e$  ( $\text{cm}^{-3}$  K) and the equipartition magnetic field  $B_{eq}$  (gauss; see eq. [3]). Note the large values of  $P$  and  $B_{eq}$  around the transition zone, caused by the impulsive heating of plasma; the value of  $B_{eq}$  there is of order 100 G.

Fig. 2. - Schematic of the flux tube interaction. Loops  $L_1$  and  $L_2$  are typical members of the same bipolar active region complex and lie across the neutral line (heavy dashed) as shown. Their magnetic fields are also twisted in the same sense due to a global active region current field  $\underline{J}$ . At some time  $t = 0$  loop  $L_1$  flares (the energy release being signified by the star at the loop apex), causing energy to flow downwards toward the chromosphere (the energy transport mechanism is here taken to be non-thermal electron bombardment, so that we may analyze its effects in some detail - see §II - however, other transport mechanisms [see §II] will have the same qualitative effect on the evolution of the system). Upon interaction with the chromosphere, the trans-

ported energy heats the plasma to very high ( $\approx 10^7$  K) temperatures, causing a large pressure enhancement at this point (see Figure 1). This causes loop  $L_1$  to expand, driving a horizontal magnetohydrodynamic disturbance (small horizontal arrows at the loop base). At some later time the surface of the disturbed field lines has the appearance  $L_1'$  (right figure; the original loop  $L_1$  is shown dashed), and is in contact with loop  $L_2$ , with the poloidal components of the magnetic fields of  $L_1'$  and  $L_2$  antiparallel in the contact plane. These components reconnect in a neutral-sheet-type scenario and cause an impulsive energy release in the hitherto quiescent loop  $L_2$ .

For the purpose of the illustration, the poloidal component of the magnetic fields has been exaggerated. Also, loop  $L_1'$  has been constructed as a simple radial dilation of loop  $L_1$ ; this is not necessarily justified in practice (see §IV).

A. GORDON EMSLIE: Institute for Plasma Research, Stanford University, Via  
Crespi, Stanford, CA 94305

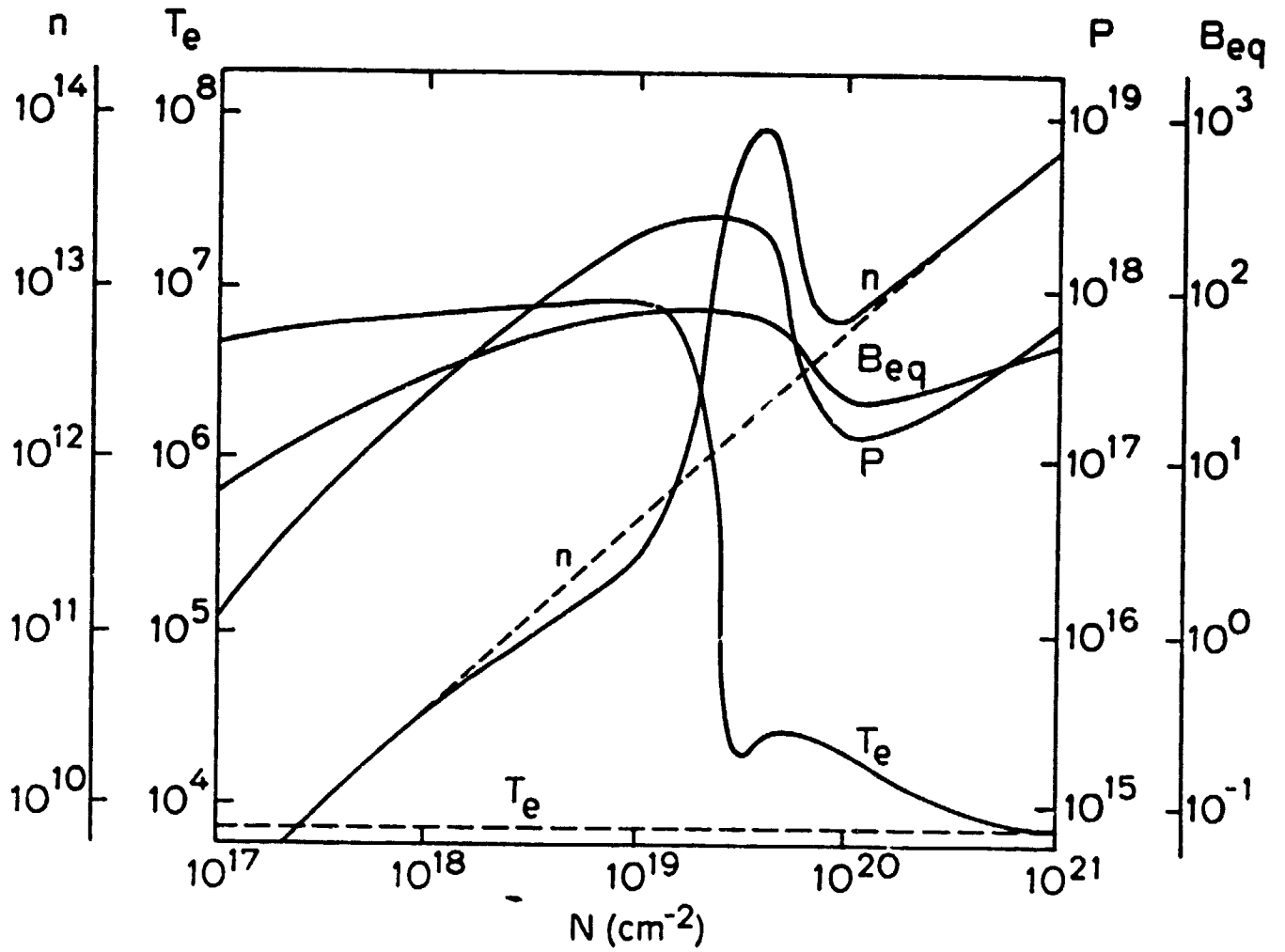


Figure 1

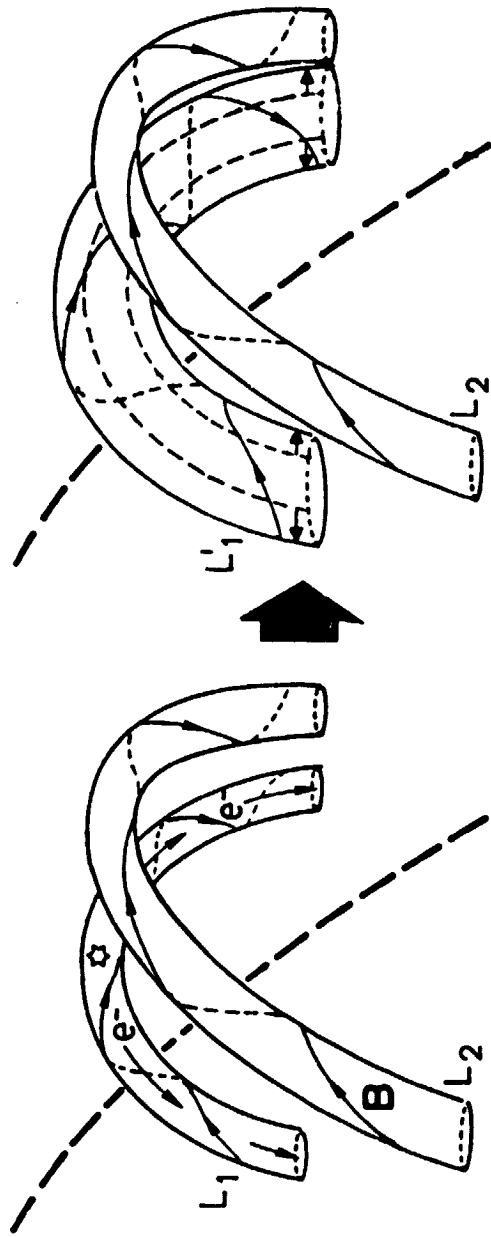


Figure 2